REFERENCE VALUE PROVISION SCHEMES FOR ATTENUATION CORRECTION OF FULL-WAVEFORM AIRBORNE LASER SCANNER DATA

K. Richter*, R. Blaskow, N. Stelling, H.-G. Maas

Institute of Photogrammetry and Remote Sensing, Technische Universität Dresden, Germany -
katja.richter1@tu-dresden.de, robert.blaskow@tu-dresden.de, nadine.stelling@tu-dresden.de, hans-gerd.maas@tu-dresden.de

Commission III, WG III/2

KEY WORDS: full-waveform airborne laser scanning, attenuation correction, waveform history analysis

ABSTRACT:

The characterization of the vertical forest structure is highly relevant for ecological research and for better understanding forest ecosystems. Full-waveform airborne laser scanner systems providing a complete time-resolved digitization of every laser pulse echo may deliver very valuable information on the biophysical structure in forest stands. To exploit the great potential offered by full-waveform airborne laser scanning data, the development of suitable voxel based data analysis methods is straightforward. Beyond extracting additional 3D points, it is very promising to derive voxel attributes from the digitized waveform directly. However, the 'history' of each laser pulse echo is characterized by attenuation effects caused by reflections in higher regions of the crown. As a result, the received waveform signals within the canopy have a lower amplitude than it would be observed for an identical structure without the previous canopy structure interactions (Romanczyk et al., 2012).
To achieve a radiometrically correct voxel space representation, the loss of signal strength caused by partial reflections on the path of a laser pulse through the canopy has to be compensated by applying suitable attenuation correction models. The basic idea of the correction procedure is to enhance the waveform intensity values in lower parts of the canopy for portions of the pulse intensity, which have been reflected in higher parts of the canopy. To estimate the enhancement factor an appropriate reference value has to be derived from the data itself. Based on pulse history correction schemes presented in previous publications, the paper will discuss several approaches for reference value estimation. Furthermore, the results of experiments with two different data sets (leaf-on/leaf-off) are presented.

1. INTRODUCTION

The scientific investigation of forest ecosystems with respect to forest-related research like carbon pools and greenhouse gas emissions (Jandl et al., 2015), silvicultural questions like lower tree crown delineation and the density of understory vegetation (Spies, 1998), as well as meteorological applications like flow simulation in forest stands (Queck et al., 2012) and gas exchange (Foken et al., 2012) require a high-resolution characterization of the vertical forest structure. Small-footprint full-waveform laser scanning systems enable the measurement of physical and geometric attributes of the vegetation canopy structure. The requested biophysical forest parameters can be derived with voxel based data - analysis methods.

In contrast to existing approaches based on the extraction of discrete 3D-points via a gaussian decomposition, it is very promising to derive the voxel attributes from the digitized waveform directly. For this purpose, the differential backscatter cross section is estimated by deconvolution techniques (Roncat et al., 2011) and projected into a Cartesian voxel structure. The voxel entries represent the amplitudes of the corresponding differential backscatter cross section. The procedure of filling the voxel space has both geometric and radiometric aspects. The geometric aspects include an intersection of the diverging laser pulse cone with the voxel structure and an interpolation procedure to obtain the actual voxel values. The differential backscatter cross section resulting from deconvolution is in first instance only an apparent cross section, because the measuring process is influenced by different attenuation effects. Therefore, the amplitudes of the backscatter cross section have to undergo some radiometric correction before being entered into the voxel structure. We currently use the received waveform instead of the differential backscatter cross section, thus implying the assumption of an infinitely short emitted laser pulse. In a next step, this has to be replaced by estimates of the differential backscatter cross section determined by proper deconvolution techniques.

There are two groups of attenuation effects which influence the emitted laser pulse and thus the shape of the received waveform and the derived differential backscatter cross section: On the one hand the attenuation due to atmospheric effects, on the other hand the attenuation of the signal during its propagation through the canopy. The former is treated in several studies (e.g. Höfle and Pfeifer, 2007; Wagner, 2010) and does not require a further discussion here. So far, the latter issue is either not considered or only considered in a very simple way. Lindberg (2012) use an iterative normalization algorithm based on the Beer-Lambert law to compensate the attenuation of the signal energy as the signal propagates through a canopy. Allouis et al. (2011) correct the aggregated waveform with a logarithmic function. Furthermore, several simulation studies contribute to an improved understanding of signal-forest interactions (Sun and Ranson, 2000; Liu et al., 2010; Pang et al., 2011; Romanczyk et al., 2012; Cawse-Nicholson et al., 2013).

In previous publications, we discussed advanced methods for attenuation correction with the goal of improving the accuracy of volumetric forest reconstructions and to enable the derivation of the biophysical structure of a forest stand from full-waveform airborne laser scanner data (Richter et al., 2014a; Richter et al., 2014b). In contrast to existing simulation studies, our investigation deals with real data (i.e. unknown tree geometry and reflectance). Our objective is to develop a correction method,

*Corresponding author.

which can be easily applied to real full-waveform forestry data sets. Therein, the correction term has to be derived from the digitized pulse echo itself. Only the recorded waveforms are available as input data. The task is achieved by analyzing the pulse history of each waveform. This analysis requires reference values which have to be estimated by appropriate methods.

The paper is divided into 5 parts. Part 2 describes the attenuation correction methods developed in previous studies, part 3 explains several approaches for reference value selection. The results of experiments with two different data sets are presented in part 4. Finally, a short conclusion is given in part 5.

2. PREVIOUS WORK

Compared to the reflection at extended targets, the propagation of an emitted laser pulse within a tree canopy is rather complex. The laser pulse interacts with different forest components such as leaves, boughs, branches and the forest floor. The echo strenght is determined by the reflectivity, size, orientation and scattering direction of a forest component. Considering the canopy as a porous medium (lower parts of the canopy are partially shaded by leaves and branches above), less photons are available for subsequent interactions. Thus, the received waveform signal within the canopy has a lower amplitude than it would be observed for an identical structure without the previous canopy structure interactions of the laser pulse (Romanczyk et al., 2013). As a result, the material in the lower parts of the canopy is underrepresented in the digitized waveform.

To receive a correct representation of the vegetation structure, the described attenuation effects have to be removed from the waveform raw data. For this purpose, the attenuation during the propagation of the laser pulse through the canopy has to be described whith a suitable model. In our previous studies, we investigated the attenuation process in simulations and practical experiments and worked out two model variants: a discrete and an integral model. The discrete attenuation model is based on the assumption that the pulse intensity is decreased at each cluster of scatterers by a certain factor which depends on the portion of the laser pulse reflected at previous interactions. The integral model is detached from the consideration of single interactions. Herein, we assume a continuous (but not linear) intensity decrease during the propagation through the canopy, also depending on previous interactions. Due to the modification of the backscattered signal shape and the resulting influence on the signal, the integral attenuation model is only valid for volumetric scatterers (leaves and branches).

According to the described attenuation models, two correction methods were developed and evaluated. The attetuation can be corrected by inverting the attenuation process. Both methods are based on the increase of the waveform intensity values in lower parts of the tree crown for portions of the pulse intensity, which have been reflected in higher parts of the crown. Hence, the attenuated received waveform can be corrected by stepwise increasing the amplitudes with an appropriate correction factor c_i. This can be done either segment-wise in discrete steps (discrete attenuation correction, fig. 1) or integral for each sample (integral attenuation correction, fig. 2). In both cases, the correction factor depends on the proportion p_i of the signal reflected at the previous interactions.

In the discrete correction method (Richter et al., 2014a), the proportion p_i is calculated by setting the area under each segment (peak) of the received waveform in relation to the reference value estimated as described in section 3. To determine the area under

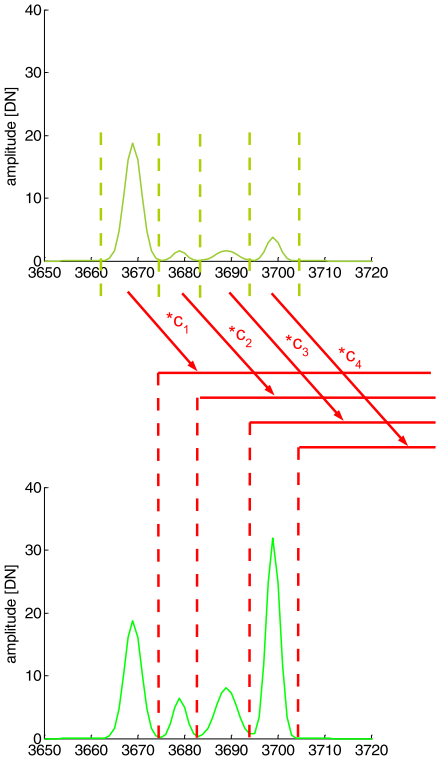

Figure 1: Discrete attenuation correction ([DN] digital number)

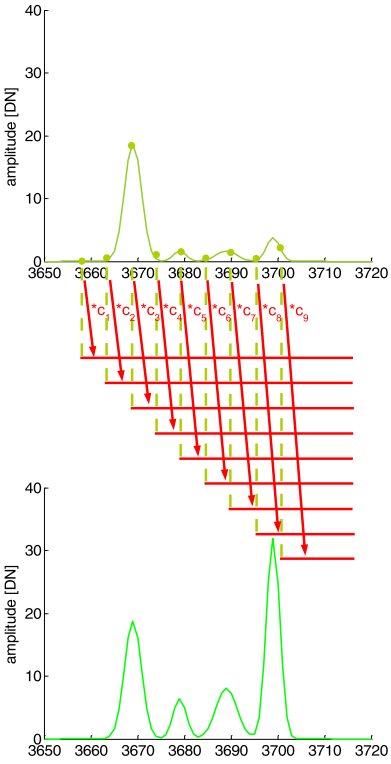

Figure 2: Integral attenuation correction

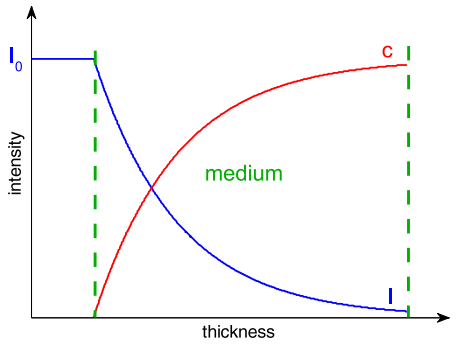

Figure 3: Beer-Lambert law with the exponential decrease of the laser pulse intensity I (blue) during the propagation through a medium (green) and corresponding correction term c (red)

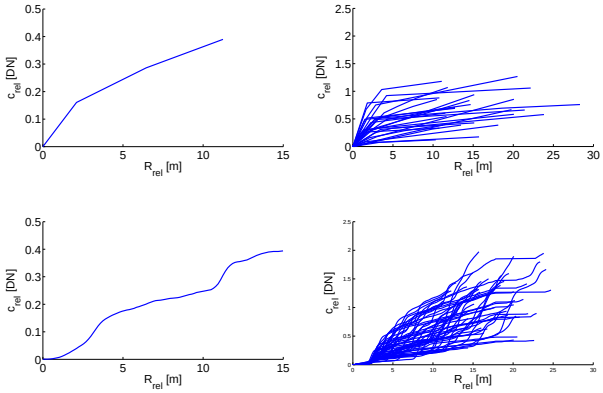

Figure 4: Relative correction factor c_{rel} as a function of relative distance R_{rel} for a single waveform (left) as well as a set of several waveforms (right), top: discrete attenuation correction, bottom: integral attenuation correction

the received waveform, the peaks and borders between the peaks have to be detected. In the integral correction method (Richter et al., 2014b), the proportion p_i is calculated as a ratio of the amplitude of the received waveform at the sample point to the reference value.

Both correction methods are based on several (in fact only confinedly valid) assumptions:

- all surfaces, which interact with the emitted laser pulse, have a similar reflectance
- leaves, boughs, branches in the footprint are randomly distributed
- the properties of the canopy can be considered in analogy to a porous medium

Nevertheless, accepting those assumptions (despite their limited validity) will usually lead to better results than applying no correction at all and simply determining forest parameters from uncorrected data. The results of our previous studies show that the quality of the volumetric forest reconstruction is considerably improved.

Our correction methods are similar to the simulation based approach of Cawse-Nicholson (Cawse-Nicholson et al., 2013), even though they are not based on the detailed consideration of single photons. The general validity of our correction models has already been proved in an experimental validation (Richter et al., 2015). Furthermore, it can easily be shown that the correction models are a refinement of the procedure presented by Lindberg (2012) . In her study she assumed an exponential decrease of the laser pulse intensity during the propagation through the canopy. Based on the Beer-Lambert law (fig. 3), she developed an iterative normalization algorithm. To illustrate the affinity of our two approaches, we plot our correction factor as a function of the distance (fig. 4). As one can see, the general course of our correction function corresponds to the correction function based on the Beer-Lambert-law (fig.3) with an individual adaption to the specific history of each pulse. About 70 % of the discrete corrected waveforms and 78 % of the integral corrected waveforms have an exponential falling course proving the physical validity of our correction models.

3. METHOD

As described in section 2, we have to estimate the proportion p_i of the signal which was reflected at the first sample to calculate the attenuation correction factor c_i. To estimate the reflected proportion, information on the energy of the incoming laser pulse is required. Although the emitted waveform is recorded in position and shape, it is not possible to calculate the incoming signal at the top of the tree. The reason is the unknown relationship between the amplitude of the digitized emitted waveform and the actually emitted energy. Therefore, another reference value is needed. Subsequently, we present three approaches deriving reference values from the recorded data sets itself.

3.1 Automatic Method

This method is based on the assumption that the incoming signal at the top of the tree corresponds to the complete reflection of the emitted signal at the forest floor. In other words, we assume that the maximal possible backscattered signal conforms to the received waveform resulting from a propagation through the canopy without any interactions. To estimate the reference value, we automatically detect all waveforms which fulfill this assumption. For this purpose, we perform a simple peak detection algorithm and extract all waveforms with a single peak. As shown in figure 5, not all single peak waveforms originate from ground reflections as some come from reflections at dense vegetation, too. A classification of the peaks with the help of the amplitudes is not possible, due to high amplitudes in the canopy resulting from interactions with thick branches and the trunk. Using the last echoes of all waveforms does not work, because many last echoes are located in the canopy, too. Therefore, we search in the point cloud for points on the forest floor whose corresponding waveforms serve as reference. For simplification reasons, we proceed scan line by scan line.

To find these points, we apply a procedure, which is similar to a simplified DTM filtering procedure: In the simplest case, each scan line is divided into two parts (fig. 5). Afterwards, we estimate the points with the highest amplitude in each part (m1 and m2), assuming that these points definitely result from reflections at the forest floor. Subsequently, the distance a to the line m1m2 is calculated for each other point. All points with a distance $a < 2\,\mathrm{m}$ are assigned to the class "forest floor", the rest to the class "canopy". In complex terrain the scan line has to be divided into more than two parts to improve the approximation of the

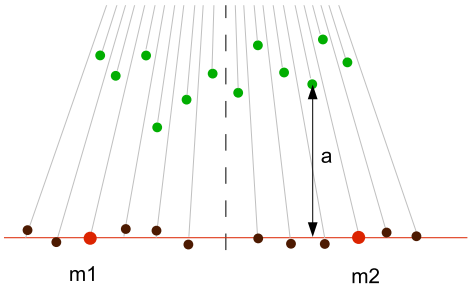

Figure 5: Classification of reference waveforms

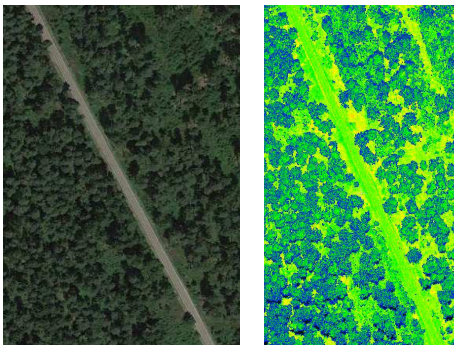

Figure 6: Asphalt road in aerial photo (left) and laser scanner point cloud (right)

ground. After the classification we extract only those points located between vegetation waveforms from all forest floor points. This way we eliminate waveforms originating from forest tracks, clearings or fields. To exclude the influence of the incidence angle, only waveforms recorded close to the nadir of the scan lines are taken into consideration. The reference value is derived from the remaining waveforms, analyzing the integrals of the signals (mean or maximum value).

The advantage of the method is the full automation as well as the fact that it can be applied on a complete data set including urban areas with roads, buildings and fields. The prerequisite for the success of the method is a sufficiently large number of laser pulses completely penetrating through the vegetation without any interactions. Due to the assumption that all surfaces, which interact with the emitted laser pulse, have a similar reflectance (sec. 2.) the reflectivity of the forest floor plays an important role. Using the forest floor waveforms for the estimation of the reference value entail that the reflectivity of the forest floor is set as common reflectivity for all materials in the footprint.

3.2 Semiautomatic Method

The forest floor is of minor relevance for the characterization of the vertical vegetation structure. Therefore, it seems reasonable to take the reflectivity of vegetation as a basis for the assumed common reflectivity of all targets. Although there are waveforms with single reflections in the canopy, those waveforms do usually not meet the requirements for reference waveforms (extended target, horizontal orientation to the scanner). Therefore, the reference value cannot be estimated reliably from those single vegetation echoes. Alternatively, we investigate the integrals of all vegetation waveforms (more than one peak). We assume that the maximal possible backscattered signal corresponds to the waveform with the highest occurring integral. This waveform results from the interaction with vegetation and forest floor and is thus influenced by attenuation effects. Therefore, the reference value is still smaller than the actual value but closer to it than the reference value derived with the automatic method in section 3.1.

Beside this advantages, the drawback of the approach is that solely vegetation waveforms may be included in the analysis of the integrals. In comparison to the first approach, the procedure has a lower automation level, as the required segmentation of a region of interest in the data set may need a certain level of user interaction. Another problem is caused by materials with very high reflectivity remaining in the segmented data set. Those materials may distort the reference value estimation and have a negative effect on the attenuation correction.

3.3 Interactive Method

This method combines the reference value estimation from echoes of extended targets with an accurate adjustment to the actual reflectivity of vegetation. The approach, requiring user interaction as well, works as follows: A point cloud is derived from the digitized waveform data with conventional methods. Afterwards, reference areas of known reflectivity ρ_{ref} are segmented manually, e.g. asphalt areas and grasslands. If possible, the reference areas should be located close to the nadir of the scan lines. Figure 6 shows a suitable asphalt road in the aerial photo and in the point cloud with color coded amplitudes. The relative reflectivity ρ_{ref} of a specific ground cover depends, among other things, on the wavelength of the used laser scanner system. Characteristic values for different types of ground cover are given in manufacturer specifications (Pfennigbauer and Ullrich, 2011). Finally, we analyze the integrals of the reference area waveforms and adapt the mean values $mean_{ref}$ to the relative reflectivity of vegetation ρ_v (Eq. 1). For better understanding we can consider the following example: The relative reflectivity ρ_{ref} of the chosen reference area is half of ρ_v. Thus, the mean value $mean_{ref}$ has to be doubled to perform the adjustment to the reflectivity of vegetation.

$$rv = mean_{ref} \cdot \frac{\rho_v}{\rho_{ref}} \tag{1}$$

The advantage here is that the reference value is close to the actual reflectivity of vegetation. Unfortunately, the method requires a high level of user interaction and is difficult to automate.Furthermore, appropriate materials with known reflectivity have to be present in the data set.

4. RESULTS AND DISCUSSION

In this section, the developed methods (sec. 3) are applied on different data sets. Our aim is to invent methods which are applicable to all kinds of forests. For the reference value estimation factors such as vegetation structure, forest species composition and foliage conditions play an important role. To ensure a structured analysis of all influences, not too many parameters should be varied at a time. First of all, we have focused on different foliage conditions. The data used for our investigations are introduced in subsection 4.1. Afterwards the results of the reference value estimation are presented and discussed.

4.1 Data

For our experiments data of two different flight campaigns have been used. The main characteristics are presented in table 1. The

	data set A	data set B
Location	Oberlausitz	Wildacker (Tharandt Forest)
Recording Time	March 2010	May 2014
Foliage	leaf-off	leaf-on
Scanner	LMS Q680	LMS Q680i
Altitude over Ground	800 m	500 m
Pulse Repitition Rate	100 kHZ	400 kHz

Table 1: Description of data sets

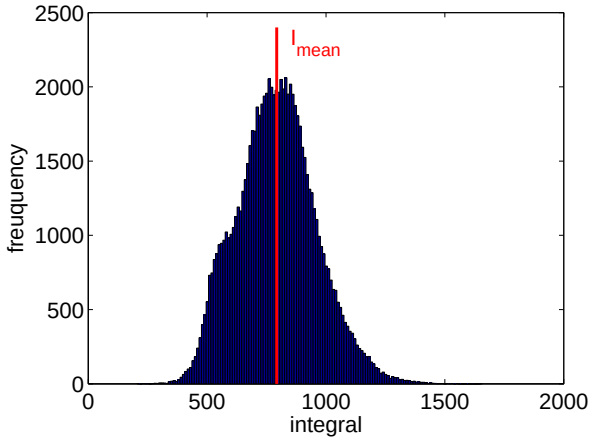

Figure 7: Histogram of the integrals of all waveforms with three interactions in the leaf-on data set

Riegl scanners used in both flight campaigns operate with the same laser having a wavelength of 1550 nm. The data sets differ with regard to foliage, flying altitude and pulse repetition rate. Due to the dependence of the amplitudes/integrals on the altitude over ground and the pulse repetition rate (Ahokas et al., 2006), the absolute values are not comparable. Although the altitude over ground is a little lower in data set B, the amplitudes are generally lower because of the considerably higher pulse repetition rate. Data set A was recorded in March 2010 in the area of Oberlausitz (Germany) under leaf-off conditions, whereas data set B, recorded in May 2014, contains fully foliated deciduous trees. To simplify the reading flow, subsequently, the data sets are termed ”leaf-off” or ”leaf-on” referring their most interesting property.

For our experiments we have selected two equally sized test regions covered with mixed forest (spruce, beech, oak, birch), which have a similar vegetation structure and forest species composition. Due to the different foliage conditions, the recorded waveforms nevertheless differ considerably. To evaluate the data, we calculate the integral and determine the number of interactions via a simple peak detection algorithm for all waveforms. The further analysis is done in classes seperated by the number of interactions. Figure 7, for example, shows the histogram of the integrals of all waveforms with three interactions in the leaf-on data set. Additionally, the mean integral ($I_{mean} = 793$) is marked.

Figure 8 shows a summary of the evaluation of all waveforms in the test regions. Each bar represents a class of waveforms with a specific number of interactions. The bar length corresponds to the number of waveforms included in the class, the position specifies the mean value of all integrals of a class. Single peak waveforms are additionally divided into forest floor and canopy. The majority of waveforms consist of one to three interactions. In the leaf-off data set, the proportion of the waveforms with more than five interactions is higher because the laser pulses can penetrate deeper into bare trees. Compared to each other, the scattering of the mean integrals of the leaf-off data set is higher than the value for the leaf-on data. This is caused by the heterogeneous characteristic and the greater variation in reflectivity (bare trees and needles vs. needles and leaves) of the leafless and indeciduous trees. Looking at the mean integrals of the individual bars, another interesting fact becomes obvious: The greater the number of interactions a waveform has before the reflection on the forest floor, the higher is the mean integral of the waveform. This is related to the different reflectivity of vegetation and forest floor. Moreover, we closely examined the single pulse waveforms by separately analyzing waveforms from ground and vegetation reflections. The comparison of the mean integral in figure 8 shows that the values for ground reflections are higher than those resulting from a single vegetation interaction. This indicates either a signal loss in the canopy or reflections at targets with a low reflectivity like branches and the trunk.

4.2 Estimation of Reference Value

We estimated the reference value with the three different methods as described in section 3 for both test regions. The results are presented in the following. In the assessment we have to take into consideration that the size of the correction factor significantly depends on the selection of the reference value. If it is too low, the correction factor becomes too large, and vice versa.

Automatic Method:

Figure 9 shows the histogram of the integrals of all eligible reference waveforms for the test regions in both data sets. In the leaf-on data set, only a small number of pulses penetrate to the ground, and even less waveforms fulfill the reference requirements. Thus, the criteria for the reference waveforms concerning the presence of vegetation waveforms in the neighborhood of a reference waveform were relieved. In both data sets the integrals differ considerably; the variance of the leaf-off data (σ =251) is higher than the variance of the leaf-on data (σ =170). Here again, the heterogeneous characteristic of the leaf-off data becomes apparent. One might either choose the mean value rv_{mean} of the areas under all eligible waveforms as reference value (leaf-off: 1516, leaf-on: 909) or the maximum value rv_{max} in one sigma distance to the mean value (leaf-off: 1767, leaf-on: 1079).

The reference value should actually be larger than the integrals of all other vegetation-waveforms because those are influenced by attenuation effects. The comparison with the histogram of all received waveforms in figure 10 shows that this is not the case. The value derived with the automatic method is more likely too small because the forest floor has mostly a lower reflectance than the leaves.

Semiautomatic Method:

The semiautomatic method requires the segmentation of a region of interest to ensure that only forest areas are included in the reference value estimation. The careful selection of the test regions makes this processing step redundant. Strictly speaking, waveforms containing reflections of the forest floor have to be eliminated. This step is currently not yet implemented.

Figure 10 shows the histogram of the integrals of all waveforms for the test regions in both data sets. As mentioned above, the leaf-off data set has more variations in the integrals and, as a consequence, a greater spread of the integrals. Nevertheless, the shape of the histograms is similar. To reduce statistical errors, we estimate the reference value in one sigma difference to the expectation value. This results in $rv = 1725$ for the leaf-off and $rv = 923$ for the leaf-on data set.

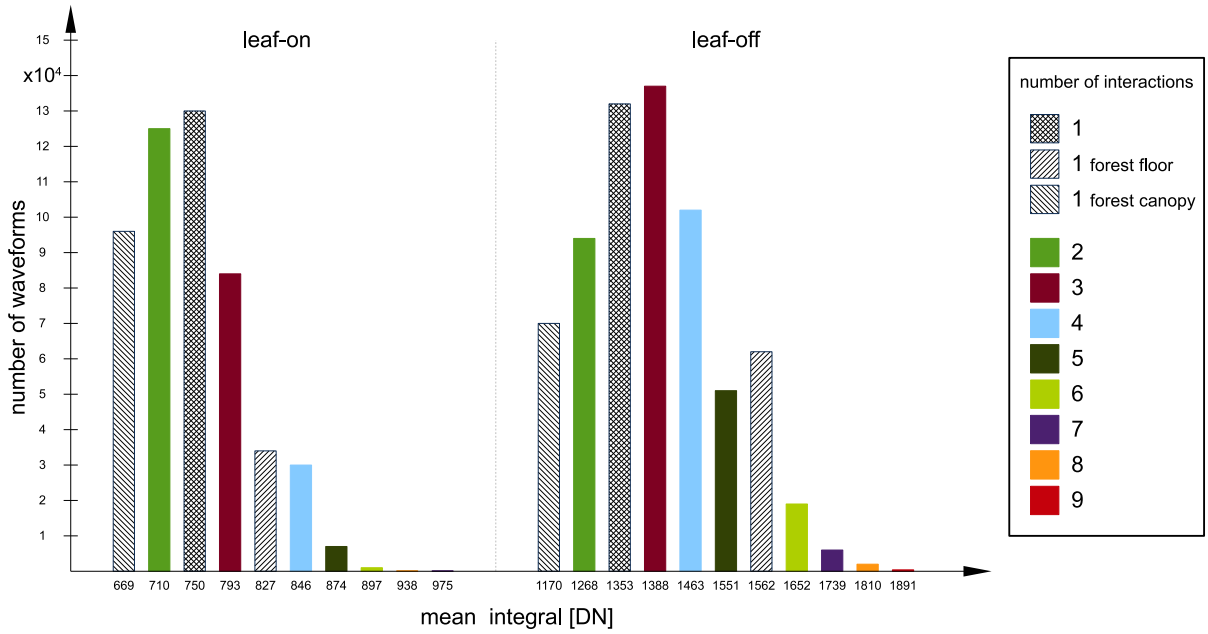

Figure 8: Summary of the evaluation of all waveforms in the test regions

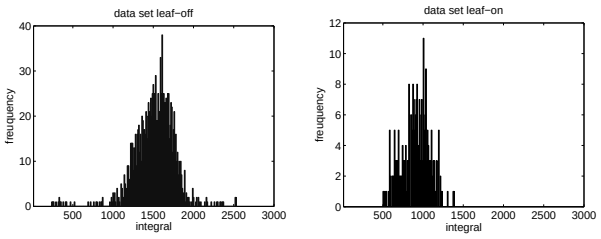

Figure 9: Histogram of the integrals of all eligable reference waveforms, left: leaf-off, right: leaf-on

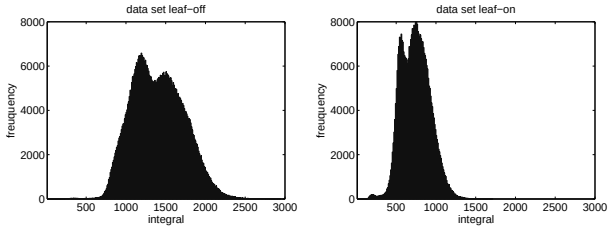

Figure 10: Histogramm of the integrals of all waveforms, left: leaf-off, right: leaf-on

As a further development, we suggest to use echoes from vegetation only. For this purpose, all waveforms with reflections from the forest floor have to be eliminated. This concerns single echoes from the ground as well as waveforms whose last echo originates from ground reflections. This procedure increases the effort for data processing, because it becomes necessary to distinguish whether a last echo originates from ground or from vegetation reflection.

Interactive Method:

To determine the reference value, we segmented several asphalt and grass areas in both data sets. In Figure 11, the histograms of the integrals of waveforms returned from asphalt respectively grass are presented for both data sets. The small variations show that the radiometric properties of the areas with the same ground cover fit together among themselves. The results of the integral analysis are presented in table 2.

The upper two lines show the mean integral values derived from the segmented areas. With the help of the relative reflectivity of asphalt and grass areas, available from manufacturer specifications, we derived a calculated value for grasslands. The comparison between measured and calculated value demonstrates the proper functioning of the reflectivity adaption. In the scanners wavelength, trees have a reflectivity of 19 % (coniferous tree) to 21 % (deciduous tree). For the correction of the whole data set, a mean reflectivity of ~22 % has to be assumed. The resulting reference values can be found in the bottom line of table 2.

4.3 Discussion

The results of the reference value estimation are summarized in table 3. The comparison shows, that the values rv_{mean} derived with the automatic method are relatively small, as expected, and do not fit well to the other ones. If the used reference value is too small, the attenuation correction factors become too large

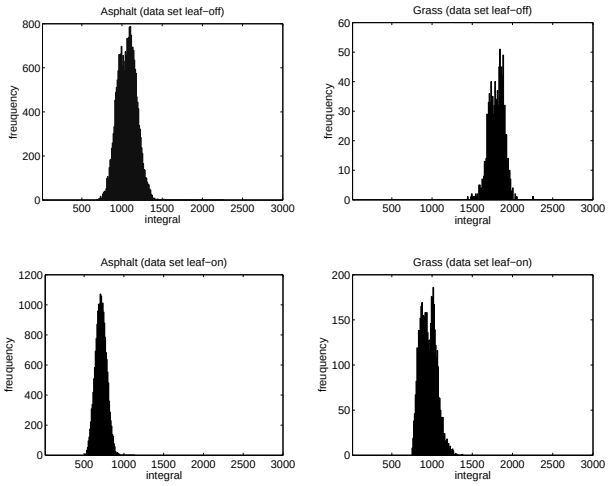

Figure 11: Histogram of the integrals of waveforms returned from asphalt respectivly grass for both data sets

	Reflectivity	leaf-off	leaf-on
Asphalt(measured)	14 %	1064	617
Grass (measured)	24 %	1816	954
Grass (calculated)	24 %	1824	1058
Tree (calculated)	∼22 %	1672	970

Table 2: Relative reflectivity, estimated mean values for both data sets and derived reference values

and cause an overcorrection. For this reason, we do not prefer rv_{mean}.

The situation is different for rv_{max}, at least for the leaf-off data set. The semiautomatic method as well as the interactive method independently deliver results similar to rv_{max}. The standard deviation of the mean value, calculated from the three independent reference values, is $\sigma = 48$. This demonstrates that the underlying assumptions are useful and valid. Things look less advantageous for the leaf-on data set, because rv_{max} considerably differ from the other two values ($\sigma = 80$). Most likely, this is not caused by shortcomings of the semiautomatic and interactive method but by the infeasibility of the automatic method to leafy regions. Due to the low number of emitted pulses penetrating to the ground without any canopy interactions as well as the simplification of the criteria for the reference waveforms, rv_{max} cannot be determined with sufficient reliability. However, the values for the leaf-on data set derived with the semiautomatic and interactive method match as well as the leaf-off values ($\sigma = 33$).

Summarizing, it can be said that the different methods lead to results with an acceptable similarity. Of course, this statement is only based on internal precision figures. An exact verification requires ground truth data. Furthermore, we have to keep in mind that the estimated reference values remain mean values for the whole data set independently of the chosen method. A specific reference value will never fit exactly to a single waveform. This is impossible due to the unknown geometry and reflectivity as well as reflectivity differences of the targets in the laser path. However, accepting the underlying assumptions and working with mean values will usually lead to a better result than determining the vegetation structure from completely uncorrected data.

Method	leaf-off	leaf-on
Automatic rv_{mean}	1516	909
Automatic rv_{max}	1767	1079
Semiautomatic	1725	923
Interactive	1672	970

Table 3: Overview of results for all methods

5. CONCLUSION

Attenuation correction of full-waveform airborne laser scanner data is still a challenging task. So far, little research has been devoted to this topic, although the solution of this problem would be a major step forward in exploiting the potential included in full-waveform data. In this study, we developed different methods to provide reference values which represent an important basis for a successful attenuation correction scheme. The reference value is derived from the data set itself at different automation levels. The experimental investigations with two different data sets demonstrate the proper functioning of the evolved approaches. Furthermore, it was shown that the methods are applicable to different foliage conditions, with minor problems with the automatic method.

In future studies, we will use multi temporal data of the same region to examine these problems closer. Furthermore, experiments are needed to investigate other factors influencing the reference value estimation (vegetation structure, forest species composition). In addition, the impact of the reference value estimation on the accuracy of the attenuation correction has to be evaluated. Avoiding the confinedly valid assumption of an infinitely short emitted laser pulse requires future work on proper deconvolution techniques.

ACKNOWLEDGEMENTS

The work presented in the paper is funded by German Research Council. We would also like to thank Aerodata Surveys and Milan Geoservices for providing the full waveform airborne laser scanner data sets used in this study.

REFERENCES

Ahokas, E., Kaasalainen, S., Hyyppä, J. and Suomalainen, J., 2006. Calibration of the optech altm 3100 laser scanner intensity data using brightness targets. International Archives of Photogrammetry, Remote Sensing and Spatial Information Sciences 36(Part 1), pp. 1–6.

Allouis, T., Durrieu, S., Véga, C. and Couteron, P., 2011. Exploiting fullwaveform lidar signals to estimate timber volume and above-ground biomass of individual trees. In: Geoscience and Remote Sensing Symposium (IGARSS), 2011 IEEE International, IEEE, pp. 1251–1254.

Cawse-Nicholson, K., van Aardt, J., Romanczyk, P., Kelbe, D., Krause, K. and Kampe, T., 2013. A study of energy attenuation due to forest canopy in small-foorprint waveform lidar signals. In: ASPRS 2013 Annual Conference Baltimore, Maryland, March 24-28, 2013.

Foken, T., Meixner, F., Falge, E., Zetzsch, C., Serafimovich, A., Bargsten, A., Behrendt, T., Biermann, T., Breuninger, C., Dix, S. et al., 2012. Coupling processes and exchange of energy and reactive and non-reactive trace gases at a forest site – results of the eger experiment. Atmospheric Chemistry and Physics 12(4), pp. 1923–1950.

Höfle, B. and Pfeifer, N., 2007. Correction of laser scanning intensity data: Data and model-driven approaches. ISPRS Journal of Photogrammetry and Remote Sensing 62(6), pp. 415–433.

Jandl, R., Bauhus, J., Bolte, A., Schindlbacher, A. and Schüler, S., 2015. Effect of climate-adapted forest management on carbon pools and greenhouse gas emissions. Current Forestry Reports, pp. 1–7.

Lindberg, E., Olofsson, K., Holmgren, J. and Olsson, H., 2012. Estimation of 3D vegetation structure from waveform and discrete return airborne laser scanning data. Remote Sensing of Environment 118, pp. 151–161.

Liu, D., Sun, G., Guo, Z., Ranson, K. J. and Du, Y., 2010. Three-dimensional coherent radar backscatter model and simulations of scattering phase center of forest canopies. Geoscience and Remote Sensing, IEEE Transactions on 48(1), pp. 349–357.

Pang, Y., Lefsky, M., Sun, G. and Ranson, J., 2011. Impact of footprint diameter and off-nadir pointing on the precision of canopy height estimates from spaceborne lidar. Remote Sensing of Environment 115(11), pp. 2798–2809.

Pfennigbauer, M. and Ullrich, A., 2011. Multi-wavelength airborne laser scanning. In: Proceedings of the International Lidar Mapping Forum, ILMF, New Orleans.

Queck, R., Bienert, A., Maas, H.-G., Harmansa, S., Goldberg, V. and Bernhofer, C., 2012. Wind fields in heterogeneous conifer canopies: parameterisation of momentum absorption using high-resolution 3D vegetation scans. European Journal of forest research 131(1), pp. 165–176.

Richter, K., Blaskow, R., Stelling, N. and Maas, H.-G., 2015. Untersuchungen zu Dämpfungseffekten in der Baumkrone bei Full-Waveform Laserscannerdaten. In: DGPF Tagungsband 24 / 2015.

Richter, K., Stelling, N. and Maas, H.-G., 2014a. Attenuation correction of full-waveform airborne laser scanner data for improving the quality of volumetric forest reconstructions by simplified waveform history analysis. In: Proceedings of the 34th EARSeL Symposium - 2nd International Workshop of Special Interest Group on Forestry, 17-18 June, Warsaw, Poland.

Richter, K., Stelling, N. and Maas, H.-G., 2014b. Correcting attenuation effects caused by interactions in the forest canopy in full-waveform airborne laser scanner data. International Archives of Photogrammetry, Remote Sensing and Spatial Information Sciences XL-3(part 3), pp. 273–280.

Romanczyk, P., Kelbe, D., van Aardt, J., Cawse-Nicholson, K., McGlinchy, J. and Krause, K., 2012. Assessing the impact of broadleaf tree structure on airborne full-waveform small-footprint lidar signals. Silvilaser Proceedings pp. 16–19.

Romanczyk, P., van Aardt, J., Cawse-Nicholson, K., Kelbe, D., Strahler, A., Schaaf, C., Krause, K. and Ramond, T., 2013. Quantifying the attenuation due to geometry interactions in waveform lidar signals. In: AGU Fall Meeting Abstracts, Vol. 1, p. 7.

Roncat, A., Bergauer, G. and Pfeifer, N., 2011. B-spline deconvolution for differential target cross-section determination in full-waveform laser scanning data. ISPRS Journal of Photogrammetry and Remote Sensing 66(4), pp. 418–428.

Spies, T. A., 1998. Forest structure: a key to the ecosystem. Northwest Science 72, pp. 34–36.

Sun, G. and Ranson, K. J., 2000. Modeling lidar returns from forest canopies. Geoscience and Remote Sensing, IEEE Transactions on 38(6), pp. 2617–2626.

Wagner, W., 2010. Radiometric calibration of small-footprint full-waveform airborne laser scanner measurements: Basic physical concepts. ISPRS Journal of Photogrammetry and Remote Sensing 65(6), pp. 505–513.